Io's Atmospheric Freeze-out Dynamics in the Presence of a Non-condensable Species

Chris H. Moore, David B. Goldstein, Philip L. Varghese, Laurence M. Trafton, Bénédicte D. Stewart, and Andrew C. Walker

The University of Texas at Austin, Department of Aerospace Engineering, 210 E. 24th St. W.R. Woolrich Laboratories, 1 University Station C0600 Austin, Tx. 78712

Abstract. One dimensional direct simulation Monte Carlo (DSMC) simulations are used to examine the effect of a trace non-condensable species on the freeze-out dynamics of Io's sulfur dioxide sublimation atmosphere during eclipse and egress. Due to finite ballistic times, essentially no collapse occurs during the first 10 minutes of eclipse at altitudes above ~100 km, and hence immediately after ingress auroral emission morphology above 100 km should resemble that of the immediate pre-eclipse state. In the absence of a non-condensable species the sublimation SO_2 atmosphere will freeze-out (collapse) during eclipse as the surface temperature drops. However, rapid collapse is prevented by the presence of even a small amount of a perfect non-condensable species due to the formation of a static diffusion layer several mean free paths thick near the surface. The higher the non-condensable mole fraction, the longer the collapse time. The effect of a weakly condensable gas species (non-zero sticking/reaction coefficient) was examined since real gas species may not be perfectly non-condensable at realistic surface temperatures. It is found that even a small sticking coefficient dramatically reduces the effect of the diffusion layer on the dynamics. If the sticking coefficient of the non-condensable exceeds ~0.25 the collapse dynamics are effectively the same as if there was no non-condensable present. This sensitivity results because the loss of non-condensable to the surface reduces the effective diffusion layer size and the formation of an effective diffusion layer requires that the layer be stationary which does not occur if the surface is a sink. As the surface temperature increases during egress from eclipse the sublimating SO_2 gas pushes the non-condensable diffusion layer up to higher altitudes once it becomes dense enough to be collisional. This vertical species stratification should alter the auroral emissions after egress.

Keywords: Io, Atmospheric Collapse, Diffusion Layer
PACS: 96.12.je, 96.12.jg, 96.30.lb

INTRODUCTION

Io's surface is partially covered with SO_2 frost that sustains a collisional sublimation atmosphere when the surface temperature is high enough (>110 K). The dayside sublimation atmosphere was expected to collapse (freeze out) during eclipse (and on the nightside) as the surface temperature drops to ~90 K, effectively halting SO_2 sublimation from the surface [1]. Thus, in addition to atmospheric variability from volcanic activity, the local sublimation SO_2 atmospheric density was expected to vary strongly depending on the local surface temperature and the presence of frost [1]. Previous 2-D computational work on Io's atmosphere has focused on modeling Io's steady-state (non-eclipse) atmosphere assuming a surface temperature as a function of the solar zenith angle (SZA) [2,3]. Simulations have found a dayside SO/SO_2 ratio of 3-7% [4], consistent with an observed ratio of 1-10% [5].[1]

While the steady state simulations are useful in determining global species concentrations, the rate at which the atmospheric column collapses upon ingress into eclipse, and in particular the response of the upper atmosphere to the collapse, is critically important for certain processes. For example, understanding Io's electrodynamic interaction with the Jupiter plasma torus during eclipse and the resulting auroral emissions requires a time-varying atmospheric model. Clarke *et al.* [6] observed the behavior of UV emissions during eclipse and found that the emission decreases

[1] SO is produced by photo-dissociation or plasma-impact dissociation of SO_2

by roughly a factor of 3 within 20 minutes of ingress. Geissler *et al.* [7] suggested that the timescale asymmetry between post-ingress dimming and egress brightening of Io's disk-averaged brightness is consistent with a partial collapse of Io's atmosphere. They infer a collapse timescale of ~20 minutes based on the observed asymmetry. Further, assuming that the sublimation atmosphere remains in equilibrium with the local surface temperature, they inferred that the atmosphere must be supported by a substantial volcanic component in order to retain the observed auroral emissions throughout eclipse. However, this assumption ignores gas dynamic processes: that the gas has a finite ballistic collapse time and that non-condensable gas species (SO, O_2) are present.

Based on previous work, the effect of even a small amount of non-condensable gas on the atmospheric freeze-out dynamics may be significant. Sone *et al.* [8] modeled a semi-infinite two species gas mixture flowing towards an infinite surface upon which one of the species condensed. Taguchi *et al.* [9] extended the analysis to a gas mixture flowing at incidence to the surface, similar to flows one might expect to find near Io's terminator. Furthermore, in the continuum limit Aoki *et al.* [10] found that even a trace amount non-condensable gas dramatically altered the flow dynamics. The non-condensable gas was found to accumulate in a Knudsen layer on the boundary, retarding condensation. Hence even a small amount of non-condensable might be expected to significantly alter Io's atmospheric collapse dynamics. However, the differences between the previously examined flows and Ionian gas dynamics (Io has a finite gas column accelerated by gravity, a surface temperature controlled sublimation rate, and the atmosphere above several kilometers altitude is rarefied) might diminish the effect of the non-condensable.

MODEL

Our computation simulates the atmospheric dynamics above a specific location (a fixed longitude and latitude) on Io's surface from the time of ingress into eclipse until after egress. The sublimation atmosphere was simulated by a one-dimensional two species (SO_2 and a non-condensable) model using the DSMC method [11]. The general details of the code and model are discussed in previous papers [2,12,13,14]. It includes an SO_2 sublimation rate based on the surface temperature, internal energy (rotation and quantized vibration) modes, and rotational and vibrational radiative cooling. The SO_2 molecules are assumed to have a unit sticking probability on the surface. The non-condensable is assumed to have a constant probability of sticking to (or reacting with) the surface. The probability ranges from 1 for a perfectly condensable gas to 0 for a perfectly non-condensable gas. If a molecule does not stick, it is assumed to scatter diffusely off the surface. The model also includes plasma heating [2], though the plasma only transfers translational and rotational energy to the target molecules. The plasma is assumed to neither dissociate nor directly excite the vibrational modes of the target molecules. Since the model does not presently account for production of SO (or O_2) from SO_2, it was necessary to artificially add the non-condensable species. Once the SO_2 sublimation atmosphere reached steady-state, the second species was added with a uniform mole fraction and then allowed to relax to quasi-steady-state. In addition, the model does not allow for destruction of SO via ion or electron impact dissociation thus the simulated SO density will be higher than the actual SO density as eclipse progresses. However, the SO lifetime for destruction near the surface is ~4 hours. Therefore the reduction in SO density due to plasma dissociation during eclipse (~2 hours) should not change the overall results dramatically.

In all cases the computational domain extended to an altitude of ~1000 km, had O(1000) cells, and had ~10^6 computational molecules (at the initial surface temperature). This resulted in >4 molecules per cell everywhere in the domain at all times during the simulations even as the surface cools and the column density drops. If a molecule crosses the top boundary, it is deleted if its velocity exceeds the escape velocity, else it is instantly reflected. The last cell is extended to high altitude (2000 km) to prevent the small number of reflected molecules (which should have come back into the domain after a short time delay) from affecting the lower atmosphere during the unsteady collapse and reformation. A range of plasma energy fluxes was investigated since the plasma torus conditions vary. However, there was little effect on the evolution of the collapse. A flux of 5 mW-m^{-2} is used for the simulations.

The surface temperature, $T_s(t)$, was obtained by solving the energy balance equation numerically:

$$\frac{d}{dt}T_s(t) = \begin{cases} \varepsilon\sigma/Mc\left(T_{s,\min}^4 - T_s^4\right) & t < \tau_{Eclipse} \\ \varepsilon\sigma/Mc\left(T_{ss}^4 - T_s^4\right) & t > \tau_{Eclipse} \end{cases}, \quad T_{ss} = \begin{cases} 30\cos^{1/4}\left(\theta(t)\right) + T_{s,\min} & \theta < 90° \\ T_{s,\min} & \theta > 90° \end{cases} \tag{1}$$

where ε is the bolometric emissivity, σ is the Stefan-Boltzmann constant, M is the local areal mass density (kg-m^{-2}), c is the specific heat of the surface, $T_{s,min}$ is the nightside temperature which was set to 90 K, T_{SS} is the steady state temperature if the moon did not rotate, and $\theta(t)$ is the SZA which varies in time since we are simulating the atmosphere above a given surface location as Io orbits Jupiter. The time spent in eclipse, $\tau_{Eclipse}$, is 120 minutes. Saur *et al.* [15] computed a value of Mc/ε equal to 350 J-m^{-2}-K^{-1} from observations [16]; however, the dynamics were

relatively insensitive to the value chosen. Thermal conduction and plasma heating of the surface have been accounted for by equating their energy transfer to the energy lost at the steady state nightside temperature, $T_{s,min}$.

RESULTS

Several cases were simulated in order to examine how the atmospheric behavior upon ingress and egress varied with the surface temperature history (and hence longitude and latitude on Io), the properties of the non-condensable species (type, concentration, and sticking probability), the plasma energy flux, and the thermal inertia of the surface. It was found that the collapse dynamics were largely independent of the plasma energy flux, the species type, and small differences in the thermal inertia. Suitable Einstein-*A* coefficients for SO radiative de-excitation from excited vibrational states were unavailable. However, the atmospheric dynamics and the resultant profiles (even vibrational temperature) were insensitive to order of magnitude changes in the Einstein-*A* value used. For the following results an Einstein-*A* value of A_{10}=10 s^{-1} was used, similar to that of CO.

Grid convergence was assured in two ways: (1) the grid size was everywhere less than the local mean free path at all times during the simulation, and (2) reducing the cell size by a factor of 2 did not change the solution. Similarly, the timestep size was chosen such that it was less than the mean time between collisions everywhere in the domain and at all times during the simulation. Note that the lifetime for de-excitation through spontaneous emission from certain excited vibrational states is smaller than our simulation timestep. To model the de-excitation correctly, it was necessary to use a finer timestep, or sub-step, which was ~10 times smaller than the de-excitation lifetime during the de-excitation routine. The sub-steps allowed for the correct distribution of vibrational states among the simulation molecules to be computed at each global simulation timestep.

Ingress (into eclipse)

Figure 1 shows the SO_2 number density, temperature, and SO mole fraction plotted as functions of altitude at three different times near the start of eclipse for an initial surface temperature of 110 K. Figure 1a shows the atmospheric response without the presence of a non-condensable (such as SO), while Fig. 1b shows the response with a non-condensable present. Note that due to the low total column density at a surface temperature of 110 K, the plasma penetrates to the surface and the gas temperature is seen to increase monotonically with altitude near the surface even as the surface temperature drops and the gas condenses. In Fig. 1a, the number density near the surface drops by ~1 order of magnitude after 10 minutes because the SO_2 vapor pressure depends on the surface temperature which is radiatively cooling during eclipse. However, the atmosphere above ~100 km remains relatively unaffected shortly after eclipse because the finite ballistic time delays the response to temperature changes at the surface.

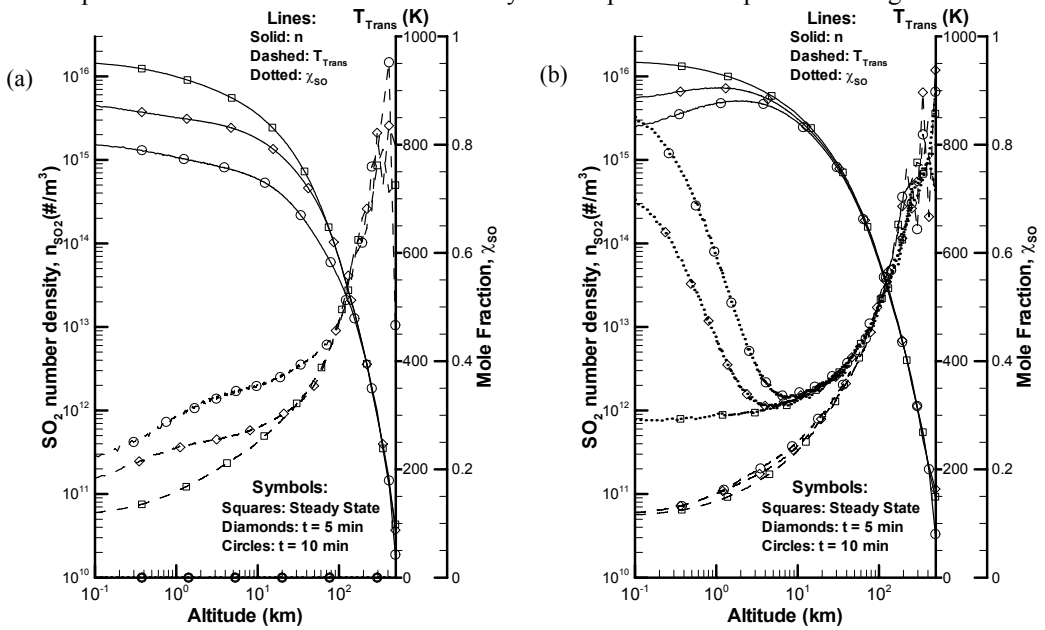

FIGURE 1. Atmosphere profiles (number density, temperature, and non-condensable mole fraction) for $T_s(t=0)$ = 110 K and (a) no non-condensable species, (b) non-condensable SO mole fraction (χ_{SO}) of 0.35 for the entire gas column.

Figure 1b shows a dramatically different result. In Fig. 1b, the SO_2 number density near the surface is seen to drop by a factor of ~5 after 10 minutes and above ~10 km there is virtually no change in SO_2 number density. Also, the gas temperature barely increases and the mole fraction of SO increases from ~29% to ~84%. The gas temperature barely changes because the total density remains nearly constant and hence the plasma energy deposition remains approximately the same. After 10 minutes the mean free path of SO_2 near the surface is ~60 m; therefore, an SO diffusion layer (an SO mole fraction greater than 50%) ~30 mean free paths high is seen to have formed. The formation of a diffusion layer prevents the SO_2 at higher altitudes from reaching the surface and slows the freeze-out of the lower SO_2 atmosphere as compared to the pure SO_2 case.

Figure 2 compares the total SO_2 column density during eclipse and shortly after egress for several different simulations; in each $T_s(t=0)$ = 110 K. If the atmospheric column remains in instantaneous equilibrium with the surface temperature, an analytic column density can be obtained from the saturation vapor pressure [17]:

$$N_{SO_2} = 1.516 \times 10^{13} \exp\left[-\frac{4510}{T_s(t)}\right] \Big/ m_{SO_2} g_{Io} \qquad (2)$$

It is seen that if there are no non-condensable species (and hence no non-condensable diffusion layer) then the DSMC simulation of the collapse of the total column lags slightly behind the equilibrium solution due to the finite ballistic collapse time. However, the simulated DSMC result with SO present lags substantially behind the equilibrium result since a relatively large amount of SO_2 is prevented from condensing by the diffusion layer. Thus the presence of a modest amount of a non-condensable species can explain the aurora intensity observed during eclipse and does not require the atmosphere to have a substantial volcanic component as previously thought [7,15].

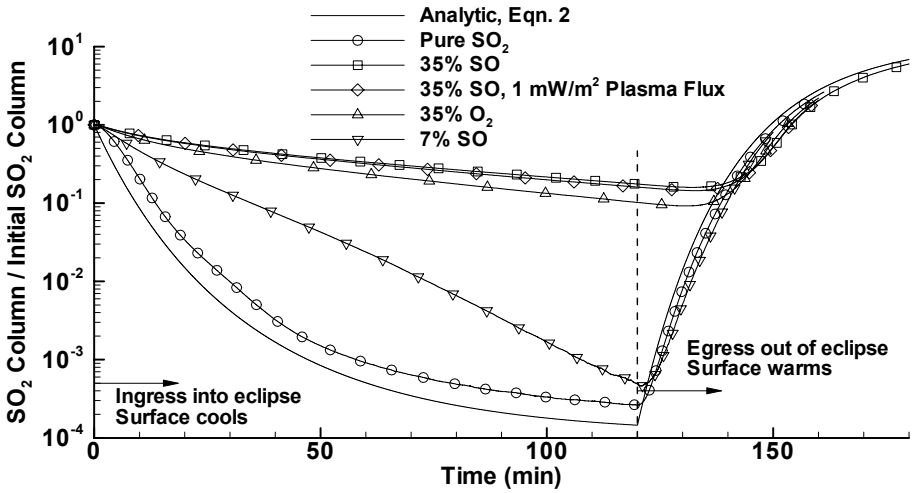

FIGURE 2. Total column density during eclipse and egress. The equilibrium SO_2 column density drops ~4 orders of magnitude during eclipse; however, the simulated result with pure SO_2 is seen to decrease somewhat slower due to the finite ballistic time which limits the altitude at which the surface temperature drop is felt. If a non-condensable gas is present, then the SO_2 column density is seen to decrease much more slowly. Note that it is the relative amount of non-condensable which controls the rate at which the SO_2 column decreases; there is virtually no difference when the plasma energy flux or the non-condensable species is changed. Immediately after egress, the column continues to decrease for the simulations with a non-condensable species.

In order to quantify the initial collapse of the atmosphere more precisely we define the collapse time, τ_c, to be the time at which the ratio of SO_2 column density to initial SO_2 column density equals e^{-1}. Only the SO_2 column was used to determine this collapse time because no substantial loss mechanism for the SO is included in the model. In order to quantify the degree of non-equilibrium of the atmosphere, the simulated collapse time is normalized by the collapse time obtained through using the surface temperature (Eq. 1) in the analytic column density (Eq. 2).

The collapse time versus the non-condensable mole fraction is shown in Fig. 3a. Not surprisingly, the collapse time increases with increasing non-condensable mole fraction. However, note that even without a non-condensable species the collapse time is longer than predicted by assuming the gas column is in equilibrium with the surface. This is due to the finite ballistic fall time which causes the upper atmospheric response to lag behind the surface changes. Based on the decrease in observed auroral emission upon ingress, the SO_2 column density collapse has been estimated to occur in ~20 minutes [6,7]. This constrains the disc averaged total non-condensable (SO, O_2, etc.) mole fraction to less than ~15% according to Fig. 3a since the majority of dayside is hotter than 110 K. However, one might expect fractional sticking or reactivity with the surface (likely for SO); therefore, in order to see the effects of partial reactivity on the collapse dynamics, the non-condensable was allowed to stick to (or react with) the

surface and be permanently lost with a fractional probability, P_{stick}, the results of which are shown in Fig. 3b. It was found that for a given initial non-condensable mole fraction, the collapse dynamics with partial condensation were very different. As seen in Fig. 3b, the atmospheric collapse time is extremely sensitive to P_{stick}; for P_{stick} >0.25 the collapse time was virtually identical to the collapse time for a pure SO_2 atmosphere despite a large initial SO mole fraction. This extreme sensitivity to the sticking coefficient has two main causes. If an SO molecule does not stick upon hitting the surface, then the upper time limit for it to return to the surface is the ballistic bounce time, or ~140 s for a 110 K surface temperature; however, collisions will tend to reduce this time. Furthermore, the fraction of non-condensable molecules lost to the ground after N impacts is $1 - (1 - P_{stick})^N$ and hence as the eclipse progresses, the number of "non-condensable" molecules available to sustain the diffusion layer decreases. For a sticking probability of 10% and ballistic bounces, roughly half of the molecules have been lost after 15 minutes (T_s = 110K) and thus the width of the diffusion layer relative to the mean free path is greatly reduced. In addition to the reduction in the diffusion layer size, a non-zero sticking probability actually prevents an effective diffusion layer from forming. For a true non-condensable (P_{stick} = 0), the formation of the diffusion layer brings the column of gas above it essentially to rest and the remaining SO_2 gas must diffuse through the layer in order to reach the surface and condense. However, for a non-zero sticking probability, the surface is still a sink for the SO and hence the SO layer retains a small vertical velocity into the surface. Thus the SO_2 gas convects to the surface instead of slowly diffusing to the surface. The SO layer near the surface then merely becomes a slow region that the SO_2 convects through, with a velocity set by the sticking probability.

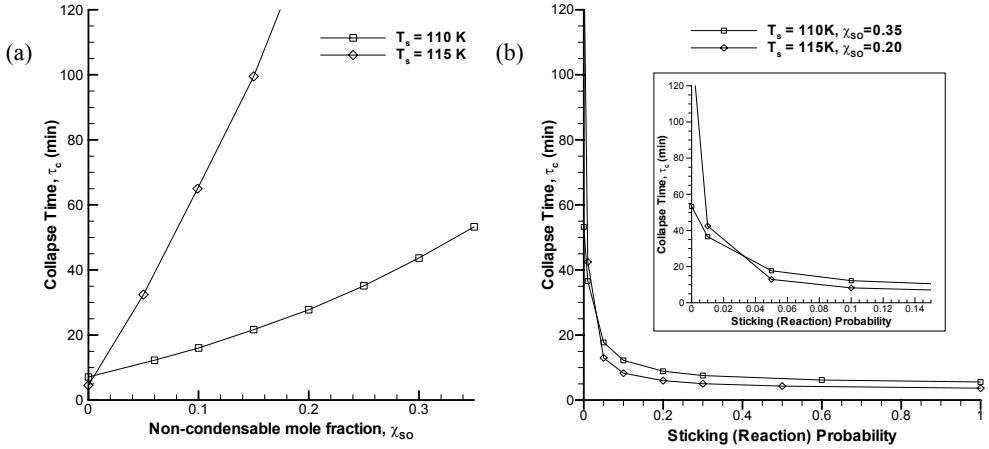

FIGURE 3. The simulated collapse time versus (a) the non-condensable mole fraction present in the total atmospheric column upon ingress and (b) the sticking (or surface reaction) probability. The non-condensable present was SO. In (a) we see that the collapse time increases rapidly with increasing mole fraction. In (b) it is found that the effect of the non-condensable on the collapse time is extremely sensitive to the non-condensable sticking coefficient. As the sticking coefficient increases, the formation of a diffusion layer is strongly hindered and the effect on atmospheric collapse decreases dramatically. Even very small sticking coefficients (~0.02) reduce the effect on the collapse time by a factor of ~2 (see inset).

Egress (out of eclipse)

The total SO_2 column density upon egress is also shown in Fig. 2. It is seen that the simulated SO_2 column density does not increase immediately upon egress and that the larger the non-condensable mole fraction is, the longer the time until the column increase begins. Thus, if post-eclipse brightening is due to atmospheric emission, then the time lag between egress and post-eclipse brightening should be indicative of the non-condensable mole fraction present. The simulated column densities continue to *decrease* for a few minutes after egress because the non-condensable diffusion layer (and to a much lesser extent the ballistic collapse time) prevents the SO_2 number density near the surface from being in equilibrium with the surface. Hence the SO_2 flux to the surface exceeds the SO_2 sublimation rate until the surface warms sufficiently. The more the SO_2 column exceeds the equilibrium value upon egress (due to the presence of a diffusion layer), the more the temperature must rise before the column can increase. Furthermore, the analytic equilibrium SO_2 column density is seen to increase throughout egress more quickly than all of the simulated cases. The slower simulated increase for the pure SO_2 column density is once again due to the finite ballistic time and the fact that at a given instant the entire column is not in equilibrium with the local surface temperature, which changes rapidly just after egress. As the surface temperature change slows, the simulated column densities are seen to approach the equilibrium value.

Figure 4a shows that the SO number density near the surface drops by a factor of ~2 over the first 20 minutes after egress, but over the next 10 minutes it drops by 2 orders of magnitude. The reason why it drops sharply after ~20 minutes is seen in Fig. 4b. At egress the SO_2-SO collision rate is negligible, but after ~15 minutes the collision rate near the surface has increased dramatically. At early times little momentum is transferred by the expanding SO_2 gas to the SO layer due to the low collision rate; the SO_2 just streams ballistically through the SO. However, as the collision rate increases, the rising SO_2 gas can no longer pass through the SO layer. The result is that the SO layer is "lifted" to higher altitudes by the SO_2 gas and the SO number density near the surface falls rapidly. Thus, the atmospheric species become segregated with nearly pure SO_2 at lower altitudes and an SO/SO_2 mixture above 10 km since the SO cannot diffuse down to lower altitudes due to the non-negligible vertical velocity. Also, as seen in Fig. 2, larger non-condensable mole fractions lead to larger differences between the equilibrium column density and the simulated column density after egress. This is because the larger the mole fraction, the more mass the subliming SO_2 must lift. Hence the SO_2 is more confined to lower altitudes and a larger number of SO_2 molecules hit the surface and stick relative to the pure SO_2 case where the SO_2 molecules are free to stream away from the surface.

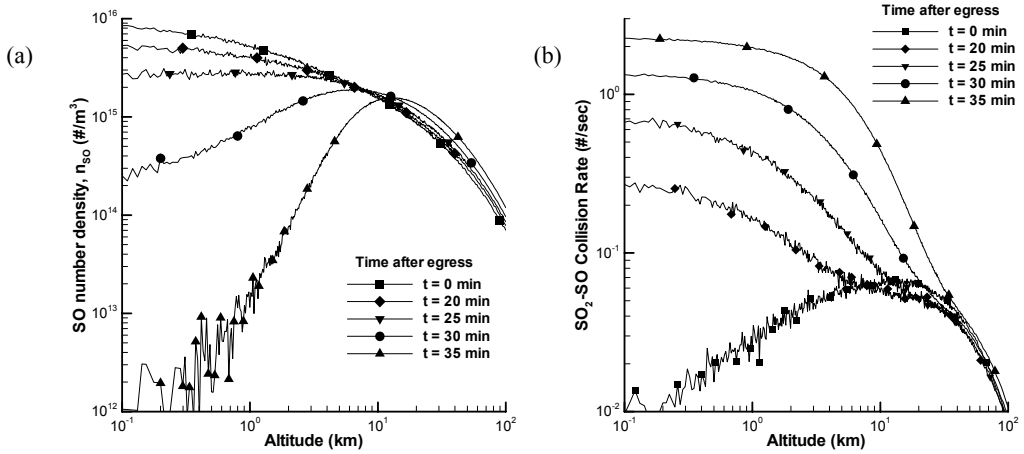

FIGURE 4. Atmosphere profiles at several times after egress for an initial eclipse surface temperature of 110K. (a) The SO number density near the surface changes very little until ~20 minutes after egress, when it drops by ~3 orders of magnitude in 15 minutes. (b) The collision rate also increases dramatically near the surface after ~15 minutes; at egress the atmosphere is nearly collisionless but becomes collisional after ~20 minutes. At early times the additional SO_2 sublimated from the surface transfers little momentum to the SO layer; however, as the collision rate increases so does the vertical momentum transfer to the SO layer. The result is that the SO number density rapidly decreases as the SO is "lifted" to higher altitudes by the sublimating SO_2 gas.

Acknowledgments: This work supported by NASA Grant NNG05G083G and NASA Grant NNX08AQ49G

REFERENCES

1. A.P. Ingersoll, *Icarus* **81**, 298-313 (1989).
2. J.V. Austin and D.B. Goldstein, *Icarus* **148**, 370-383 (2000).
3. W.H. Smyth and M.C. Wong, *Icarus* **171**, 171-182 (2004).
4. M.C. Wong and W.H. Smyth, *Icarus* **146**, 60-74 (2000).
5. K.L. Jessup, J.R. Spencer, G.E. Ballester, R.R. Howell, F. Roesler, M. Vigel, and R. Yelle, *Icarus* **169**, 197-215 (2004).
6. J. Clarke, J. Ajello, J. Luhmann, N. Schneider, and I. Kanik, *JGR* **99**, No. E4, 8387-8402 (1994).
7. P. Geissler, A. McEwen, C. Porco, D. Strobel, J. Saur, J. Ajello, and R. West, *Icarus* **172**, 127-140 (2004).
8. Y. Sone, K. Aoki, and T. Doi, *Transp. Theory Stat. Phys.* **21**, 297-328 (1992).
9. S. Taguchi, K. Aoki, and S. Takata, *Physics of Fluids* **15**, 689-705 (2003).
10. K. Aoki, S. Takata, and S. Taguchi, *Eur. J. Mech. B/Fluids* **22**, 51-71 (2003).
11. G.A. Bird, *Molecular Gas Dynamics and the Direct Simulation of Gas Flows*, Oxford: Oxford Univ. Press., 1994.
12. J. Zhang, D.B. Goldstein, P.L. Varghese, N.E. Gimelshein, S.F. Gimelshein, and D.A. Levin, *Icarus* **163**, 182-197 (2003).
13. J. Zhang, D.B. Goldstein, P.L. Varghese, L. Trafton, C. Moore, and K. Miki, *Icarus* **172**, 479-502 (2004).
14. C.H. Moore, D.B. Goldstein, P.L. Varghese, L.M. Trafton, B.D. Larignon, and A.C. Walker, *LPSC XXXVII*, **2266** (2006).
15. J. Saur and D.F. Strobel, *Icarus* **171**, 411-420 (2004).
16. W. Sinton and C. Kaminski, *Icarus* **75**, 207-232 (1988).
17. D. Wagman, Sublimation Pressure and Enthalpy of SO_2, Chem. Thermodyn. Data Cent., Natl. Bur. Of Stand., (1979).